Unsteady ship waves observed both on the ship and at sea

Xiaobo Chen[1] and **Hui Liang**[2]

[1]Research Department, Bureau Veritas Marine & Offshore, Paris, France
[2]Technical Centre for Offshore and Marine, Singapore (TCOMS), 118411, Singapore

xiao-bo.chen@bureauveritas.com

Further to the work by Liang et al (2023) on *steady* ship waves from the perspective of an earth-fixed observer, we describe here time-harmonic *unsteady* ship waves observed at sea, i.e., at a fixed point, in addition to the usual observation on the ship. The results obtained in the translating coordinate system fixed with the ship, summarized in Chen & Noblesse (1997), are used to reveal different features in the earth-fixed coordinate system. Furthermore, the heat map of time-harmonic ship waves is obtained by the analysis based on the time-frequency spectrograms.

1 Introduction

Same as steady ship waves, time-harmonic flows around a ship advancing in waves are usually described in the coordinate system moving with the ship's average speed. Within this moving reference system, detailed descriptions of ship waves have been made in many previous studies. Following the decomposition of free-surface effects into wave and local components given in Noblesse & Chen (1995), recent works by Noblesse (2000) and Chen (2004) revealed that essential physical features such as different wave systems and their wavelengths, cusp angles, phase, and group velocities, are directly related to wavenumber curves (also called dispersion curves) determined by the dispersion relation on the mathematical Fourier plane. Insightful physical results have been achieved and applied in developing numerical tools to predict ship seakeeping.

However, the description of time-harmonic ship waves in the earth-fixed coordinate system is missing although a few studies exist on steady ship waves like that by Liang et al (2023). It is not as trivial as expected, to transform results in the moving coordinate system to the fixed coordinate system. Much caution is needed to obtain consistently the phase and group velocities which are closely associated with wave crestlines. In the present study, after having summarized the classical results in the moving coordinate system, important analyses of time-harmonic ship waves in the earth-fixed coordinate system are presented with numerical illustrations. The results obtained in both coordinate systems are believed to be useful in the prediction of ambient waves due to the passage of ships.

2 Mathematical formulations

We define a Cartesian coordinate system $(O-XYZ)$ fixed on earth by choosing its (X,Y) plane to coincide with the undisturbed free surface and the $Z-$axis oriented positively upward, and a moving coordinate system $(o-xyz)$ in parallel with $(O-XYZ)$ but to move at the same constant speed as the ship along the positive x direction. The relationship between these two coordinate systems is given by

$$x = X + X_0 - U(T - T_0), \quad y = Y + Y_0, \quad z = Z \tag{1}$$

in which (X_0, Y_0) are the coordinates of the origin o at the instant T_0. The constants (X_0, Y_0, T_0) are usually put to be zero or $X_0 = -UT_0$ & $Y_0 = 0$, for the sake of simplicity.

In the moving coordinate system translating at the speed $F_{\rm r} = U/\sqrt{gL}$ scaled with the acceleration due to gravity g and ship length L, the time-harmonic ship waves at some distance from the ship represented by a point source of unit density at the origin pulsating with a frequency ω_e are usually expressed by

$$\Phi(x, y, z, t) = \Re\mathrm{e}\left\{\phi(x, y, z)\mathrm{e}^{-\mathrm{i}\omega t}\right\} \tag{2}$$

with the scaled frequency $\omega = \omega_e\sqrt{L/g}$ and $t = T\sqrt{g/L}$. The wave component $\phi(x, y, z)$ is given in Noblesse & Chen (1995) by a single integral

$$\phi = \frac{1}{4\pi\mathrm{i}} \int_{D=0} \mathrm{d}s \left[\mathrm{sgn}(D_\omega) + \mathrm{sgn}(xD_\alpha + yD_\beta)\right] \frac{\mathrm{e}^{kz}}{\|\nabla D\|} \mathrm{e}^{-\mathrm{i}(\alpha x + \beta y)} \tag{3}$$

where the dispersion function $D(\alpha, \beta, \omega, F_{\rm r})$ is defined in the Fourier plane (α, β) as the real part of the complex dispersion function $\mathcal{D}(\alpha, \beta, \omega, F_{\rm r}, \epsilon)$ given as (eq. 32) in Chen (2023) including viscous effects :

$$D = (\omega - F_{\rm r}\alpha)^2 - k = \lim_{\epsilon \to 0^+} \mathcal{D}(\alpha, \beta, \omega, F_{\rm r}, \epsilon) \tag{4}$$

with $k = \sqrt{\alpha^2 + \beta^2}$, and its derivatives

$$D_\omega = 2(\omega - F_{\rm r}\alpha) \; ; \quad D_\alpha = -2F_{\rm r}(\omega - F_{\rm r}\alpha) - \alpha/k \quad \text{and} \quad D_\beta = -\beta/k \tag{5}$$

and $\|\nabla D\| = \sqrt{D_\alpha^2 + D_\beta^2}$. The integral increment $\mathrm{d}s$ is the arc length along the wavenumber curves in the Fourier plane (α, β) defined by the dispersion equation $D = 0$. There are several curves depending on the parameter $\tau = \omega F_\mathrm{r}$, typically three distinct dispersion curves: an open one on the left ($\alpha < 0$), another open on the right ($\alpha > 0$) and a closed one around the origin for $\tau < 1/4$, the left open curve touching the closed one for $\tau = 1/4$ and becoming only one open curve for $\tau > 1/4$ together with the open curve on the right ($\alpha > 0$). Associated with these distinct dispersion curves, the outer-V, inner-V and ring waves for $\tau < 1/4$, and ring-fan and inner-V waves for $\tau > 1/4$, respectively, are nominated in Chen & Noblesse (1997), Noblesse (2000) and Chen (2004).

By using the polar coordinates both in the Fourier plane $(\alpha, \beta) = k(\cos\theta, \sin\theta)$ and on the free surface $(x, y) = h(\cos\gamma, \sin\gamma)$, the phase function in (3) is then written as

$$\psi = \alpha x + \beta y = kh\cos(\theta - \gamma) \tag{6}$$

The stationary phase defined by $\psi' = \alpha' x + \beta' y = 0$ yields the relation

$$xD_\beta - yD_\alpha = 0 = h\|\nabla D\|\sin(\vartheta - \gamma) \tag{7}$$

obtained by using $D_\alpha \alpha' + D_\beta \beta' = 0$ along $D = 0$. In above (7), $\vartheta = \arctan(D_\beta / D_\alpha)$ represents the angle between the unit vector normal to the dispersion curve and the α-axis. The equation (7) shows that the vector (x, y) is parallel to the vector (D_α, D_β) at the right angle to the dispersion curve at the point of the stationary phase. Indeed, $\vartheta = \gamma$ if $\mathrm{sgn}(D_\omega) = 1$ or $\vartheta = \pi + \gamma$ if $\mathrm{sgn}(D_\omega) = -1$ due to the fact that $xD_\alpha + yD_\beta$ is just the dot product of vectors (x, y) and (D_α, D_β) so that $\mathrm{sgn}(xD_\alpha + yD_\beta)$ must be the same sign as $\mathrm{sgn}(D_\omega)$ for the integrand function in (3) to make sense. The asymptotic expression of (3) is then given by

$$\phi(x, y, z) \approx \sum_{s=1}^{2,3} \frac{1}{\mathrm{i}\sqrt{2\pi h|\psi_s''|}} \frac{\mathrm{e}^{k_s z}}{\|\nabla D_s\|} \mathrm{e}^{-\mathrm{i}(\alpha_s x + \beta_s y) - \mathrm{sgn}(\psi_s'')\mathrm{i}\pi/4} \tag{8}$$

in which ψ_s'' is the second derivative of the scaled phase function (ψ/h) at the stationary points (α_s, β_s) along the two (for $\tau < 1/4$) or three (for $\tau > 1/4$) dispersion curves. The asymptotic expression (8) is valid for $|\psi_s''| > 0$ in which case the lines of constant phase, for example, $\psi = \alpha x + \beta y = \mp n(2\pi)$ with integers $n > 0$, are drawn by

$$(x, y)_n = \pm 2n\pi (D_\alpha, D_\beta)/(\alpha D_\alpha + \beta D_\beta) \tag{9}$$

derived from (7) with (D_α, D_β) defined by (5) at the stationary points (α_s, β_s). The sign $\pm$ in (9) should be consistent with the sign of $\mathrm{sgn}[D_\omega(\alpha D_\alpha + \beta D_\beta)]$. The crestlines (9) associated with a series of constant phases are depicted on the right of Figure 1 and well representative to wave patterns obtained by (8) depicted on the left of Figure 1.

The second derivative of the phase function can be evaluated as

$$\psi''/h = \alpha'' \cos\gamma + \beta'' \sin\gamma = c\,\left[(\alpha')^2 + (\beta')^2\right] \sin(\vartheta + \gamma)/\sin 2\vartheta \tag{10}$$

where $c = (2D_{\alpha\beta} D_\alpha D_\beta - D_{\alpha\alpha} D_\beta^2 - D_{\beta\beta} D_\alpha^2)/\|\nabla D\|^3$ is the curvature of dispersion curves at the point of stationary phase. Thus $\psi_s'' = 0$ at the stationary point where the curvature $c = 0$ is often called the inflection point, and the angle $\vartheta = \vartheta_c$ of the normal vector is maximum. According to (7), time-harmonic ship waves should be contained within the angles $\pm\gamma_c$ measured from the negative $x-$axis with $\gamma_c = \pi - \vartheta_c$ written by

$$\gamma_c = \pi - \arctan(D_\beta/D_\alpha)|_{c=0} = \arcsin(1/\sqrt{6F_\mathrm{r}^2 k_c}) \tag{11}$$

in which the wavenumber k_c satisfies

$$F_\mathrm{r}^4 k_c^2 - (3/2)F_\mathrm{r}^2 k_c + \mathrm{sgn}(D_\omega) 4\tau F_\mathrm{r}\sqrt{k_c} - 3\tau^2 = 0 \tag{12}$$

derived from $c = 0 = D$. It is noted in Chen (2004) that (11) is valid for all wave systems except for the cusp angle of the ring-fan waves in the interval of $\tau \in (1/4, \sqrt{2/27})$ which is equal to its complement to π. Several particular values of γ_c for different τ are listed in Table 1 (page 376) in Chen (2004).

According to the definition (2) and the asymptotic expression (8), the phase velocity $\boldsymbol{v}_p$ representing the change rate of phase function is given by

$$\boldsymbol{v}_p = -(\alpha_s, \beta_s)\omega/k^2 = -(\cos\theta, \sin\theta)\omega/k \tag{13}$$

which is at the right angle to the crestlines defined by (9). The negative sign in (13) is consistent with the phase definition (6) such that the direction of the phase change rate is opposite to that of the wavenumber vector $(\alpha, \beta)/k =$

$(\cos\theta, \sin\theta)$ The phase velocity (13) has its magnitude $|\boldsymbol{v}_p| = \omega/k$. On the other side, the group velocity at which wave energy propagates is defined by

$$\boldsymbol{v}_g = -(\partial\omega/\partial\alpha, \partial\omega/\partial\beta) = (D_\alpha, D_\beta)/D_\omega = -(F_\mathrm{r}, 0) - \mathrm{sgn}(D_\omega)(\alpha, \beta)/(2k^{3/2}) \tag{14}$$

which is in the radial direction from the origin in parallel with the normal vector defined by $(D_\alpha, D_\beta)/\|\nabla D\|$ of the dispersion curves at the stationary point. It can be checked that the dot product

$$(x, y)_n \cdot \boldsymbol{v}_g = 2n\pi(D_\alpha^2 + D_\beta^2)/|D_\omega(\alpha D_\alpha + \beta D_\beta)| > 0 \tag{15}$$

which shows that wave energy is propagating away from the disturbance in accordance with the radiation condition.

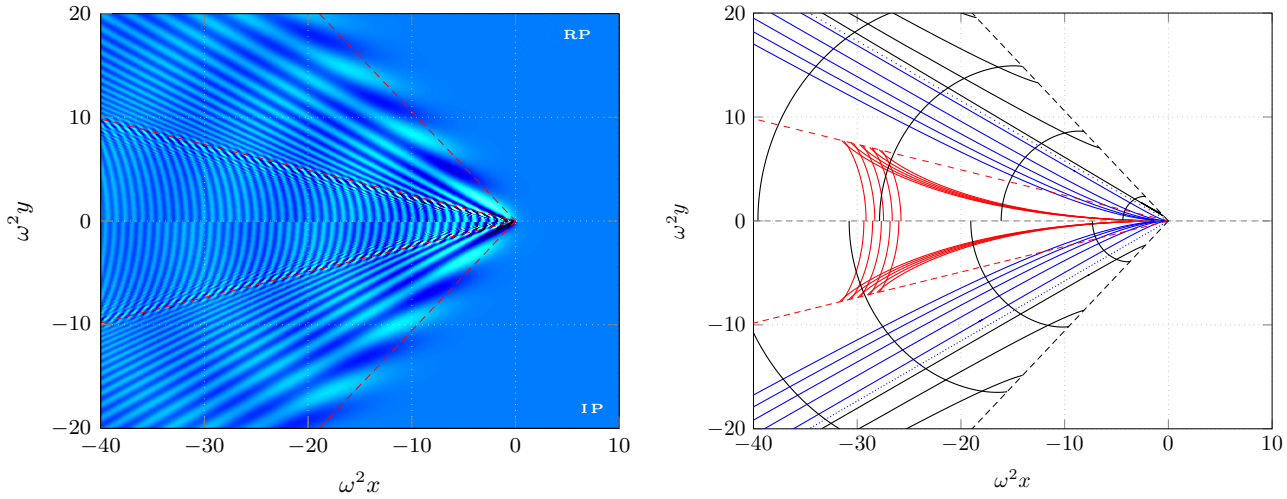

Figure 1: Wave patterns (left) and crestlines (right) for $\tau = 0.5$

Now we analyze the above features of time-harmonic ship waves in the earth-fixed coordinate system. The time (t), wavenumbers (k) and relative positions of wave systems (crestlines) are invariant. They keep the same as those in the moving coordinate system, just like that the same picture taken in one instant centered at ship's position is now observed at another position of some distance behind the ship. However, many things change. Firstly, the expression (2) of waves is now written by

$$\Phi(X, Y, Z, t) = \Re\mathrm{e}\left\{\phi(X, Y, Z)\mathrm{e}^{-\mathrm{i}\Omega t}\right\} \tag{16}$$

in which the frequency Ω is given by

$$\Omega = \omega - F_\mathrm{r}\alpha = \omega - F_\mathrm{r}k\cos\theta \tag{17}$$

obtained by introducing (1) in (8) and (2), and using the scaled speed, frequency and time. The dispersion equation (4) becomes then

$$D = 0 = \Omega^2 - k \tag{18}$$

Secondly, the phase velocity in the earth-fixed coordinate system is changed as

$$\boldsymbol{V}_p = \boldsymbol{v}_p - (\cos\theta, \sin\theta)F_\mathrm{r}(-\cos\theta) = -(\cos\theta, \sin\theta)\Omega/k \tag{19}$$

by considering the component of forward speed in the direction at right angle to wave crests. On the other side, the group velocity is then

$$\boldsymbol{V}_g = \boldsymbol{v}_g + (F_\mathrm{r}, 0) = -\mathrm{sgn}(D_\omega)(\cos\theta, \sin\theta)/(2\sqrt{k}) \tag{20}$$

From (18), we have $\Omega = \mathrm{sgn}(D_\omega)\sqrt{k}$ so that

$$\boldsymbol{V}_g = \frac{1}{2}\boldsymbol{V}_p \tag{21}$$

The group velocity is just the half of phase velocity, consistent with kinematic characteristics of free-surface waves in deep water. Both group and phase velocities are oriented in the wave-propagation direction at right angle to wave crests.

Thirdly, unlike the time-harmonic ship waves observed on the ship oscillating at a unique frequency ω, the ship waves represented by $\Phi(X, Y, Z, t)$ and defined by (16) at a fixed point $(X = X_0, Y = Y_0, Z = 0)$ at sea are composed of a series of wave frequencies Ω defined by (17). The frequency Ω is again dependent on the time t since $k\cos\theta$ associated with $x = X_0 - F_\mathrm{r}t$ is different for a different time t with a fixed point (X_0, Y_0).

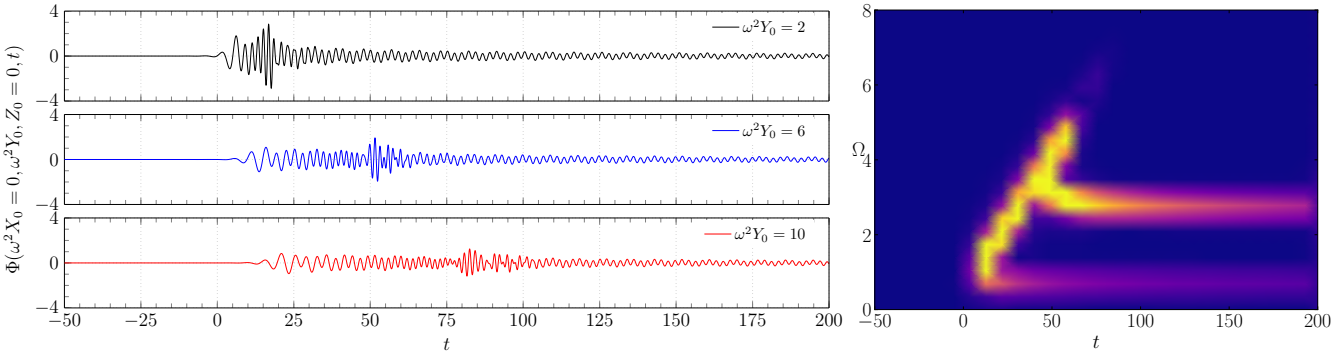

Figure 2: Time series (left) of time-harmonic ship waves for $\tau = 0.5$ at $\omega^2 X_0 = 0$ and $\omega^2 Y_0 = 2, 6$ and 10, and its time-frequency spectrograms (right) for $\omega^2 Y_0 = 6$.

3 Discussion and conclusions

The time series (16) measured at a fixed point (X_0, Y_0) are depicted on the left of Figure 2 for $X_0 = 0$ and $\omega^2 Y_0 = 2, 6$ and 10. The method based on time-frequency spectrograms developed in Liang et al (2023) is applied to analyze time series of these unsteady short-crested waves. One of the "heat" maps for $\omega^2 Y_0 = 6$ is illustrated on the right of Figure 2. Unlike steady ship waves whose time-frequency spectrograms present only one continuous band of L-shaped *boomerang* with two wings (branches) including horizontal one (transverse waves) and an oblique one (divergent waves), here we have two boomerangs. The one on the top-right part resembling that of steady ship waves is the inner-V waves, with the highest spectrum at $t \approx 49$ when the cusp is touched at $\omega^2 Y_0 = 6$. The one on the lower part is associated with ring-fan waves: the horizontal branch at very low frequency corresponding to partial ring waves and the oblique branch with increasing frequency linked to the fan waves. The two branches of ring-fan waves join at $t \approx 11$ when the cusp is touched at $\omega^2 Y_0 = 6$. More information like the slope of oblique branches, and nodes where spectrum values are minimum along the oblique branches of divergent waves and fan waves, as well as along the partial-ring waves, is also insightful to derive physical properties of unsteady ship waves.

Here, we have summarized some important features of time-harmonic ship waves observed both on the ship in the moving coordinate system, and at sea in the earth-fixed coordinate system. Major differences are that waves observed at sea have a series of frequencies depending on the measurement position and time (X_0, Y_0, t), and that the phase and group velocities have different relationships than those evaluated on the ship. Although only the velocity potential $\Phi(X, Y, Z, t)$ is considered, the extension to wave elevations $\eta(X, Y, t)$ is direct and wave elevations have the same characteristic features. The real ship waves depending on the ship's hull which can be represented by a distribution of sources need more elaborated solutions of seakeeping of a ship advancing in waves. These time-harmonic ship waves are added to the usual steady ship waves plus incoming waves. Their analyses separately or/and together are challenging but very interesting.

Acknowledgments

H.L. is supported by the National Research Foundation, Singapore and Singapore Maritime Institute under the Maritime Transformation Programme White Space Fund (Centre of Excellence for Autonomous and Remotely Operated Vessels (CEAOPS), Project ID SMI-2019-MTP-01).

References

[1] Liang H., Li Y. & Chen X.B. (2023) Physical properties of the ship wake and its detection. *38th IWWWFB*, Michigan.

[2] Chen X.B. & Noblesse F. (1997) Dispersion relation and far-field waves. *12th IWWWFB*, Carry-Le-Rouet.

[3] Noblesse F. & Chen X.B. (1995) Decomposition of free-surface effects into wave and near-field components. *Ship Technology Research* (42), 167-185.

[4] Noblesse F. (2000) Analytical representation of ship waves (23rd Weinblum Memorial Lecture), 1-35.

[5] Chen X.B. (2004) Analytical features of unsteady ship waves. *In Advances in Engineering Mechanics – Reflections and Outlook, World Scientific Publishing*, pp371-89.

[6] Chen X.B. (2023) Fundamental solutions to ship-motion problems with viscous effects. *Physics of Fluids* (35).